

See discussions, stats, and author profiles for this publication at: <https://www.researchgate.net/publication/5579691>

# Diffraction Micro Bar Codes for Encoding of Biomolecules in Multiplexed Assays

ARTICLE *in* ANALYTICAL CHEMISTRY · MARCH 2008

Impact Factor: 5.64 · DOI: 10.1021/ac7018574 · Source: PubMed

CITATIONS

24

READS

42

14 AUTHORS, INCLUDING:



**Gabriel Cavalli**

University of Surrey

23 PUBLICATIONS 301 CITATIONS

SEE PROFILE



**David Holmes**

Sphere Fluidics Ltd.

75 PUBLICATIONS 1,046 CITATIONS

SEE PROFILE



**Cameron Neylon**

29 PUBLICATIONS 832 CITATIONS

SEE PROFILE



**Peter Roach**

University of Southampton

77 PUBLICATIONS 2,286 CITATIONS

SEE PROFILE

# Diffractive Micro Bar Codes for Encoding of Biomolecules in Multiplexed Assays

Graham R. Broder,<sup>†</sup> Rohan T. Ranasinghe,<sup>†</sup> Joseph K. She,<sup>†</sup> Shahanara Banu,<sup>†,‡</sup> Sam W. Birtwell,<sup>§,||</sup> Gabriel Cavalli,<sup>†</sup> Gerasim S. Galitonov,<sup>§</sup> David Holmes,<sup>‡</sup> Hugo F. P. Martins,<sup>†</sup> Kevin F. MacDonald,<sup>§</sup> Cameron Neylon,<sup>†,⊥</sup> Nikolay Zheludev,<sup>§</sup> Peter L. Roach,<sup>\*,†</sup> and Hywel Morgan<sup>\*,‡</sup>

School of Chemistry, School of Electronics and Computer Science, Optoelectronics Research Centre, and School of Physics and Astronomy, University of Southampton, Highfield, Southampton, SO17 1BJ, UK, and STFC, Rutherford Appleton Laboratory, Didcot, OX11 0QX, UK

Microparticles incorporating micrometer-sized diffractive bar codes have been modified with oligonucleotides and immunoglobulin Gs to enable DNA hybridization and immunoassays. The bar codes are manufactured using photolithography of a chemically functional commercial epoxy photoresist (SU-8). When attached by suitable linkers, immobilized probe molecules exhibit high affinity for analytes and fast reaction kinetics, allowing detection of single nucleotide differences in DNA sequences and multiplexed immunoassays in <45 min. Analysis of raw data from assays carried out on the diffractive microparticles indicates that the reproducibility and sensitivity approach those of commercial encoding platforms. Micrometer-sized particles, imprinted with several superimposed diffraction gratings, can encode many million unique codes. The high encoding capacity of this technology along with the applicability of the manufactured bar codes to multiplexed assays will allow accurate measurement of a wide variety of molecular interactions, leading to new opportunities in diverse areas of biotechnology such as genomics, proteomics, high-throughput screening, and medical diagnostics.

Rapid and multiplexed molecular detection with high sensitivity and specificity is of great importance in gene profiling, clinical diagnostics, and environmental monitoring. A key requirement for multiplexing is the identification of each molecule set within the library of probes used in an assay. In this context, microarrays have revolutionized DNA expression profiling<sup>1,2</sup> and show great promise for proteomics<sup>3–6</sup> and DNA sequencing.<sup>7</sup> In these

systems, a large number of different biomolecules are identified by their position on a two-dimensional grid. However, microarrays have certain disadvantages, including slow diffusion of molecules to their binding sites and the inability to perform large numbers of reactions simultaneously over a wide dynamic range.

Bead or suspension arrays, in which probes are attached to the surface of microparticles, are an attractive alternative for multiplexed analysis and have found applications in profiling DNA or proteins from complex biological samples.<sup>8,9</sup> Such arrays offer a number of advantages, including fast reaction kinetics and flexibility of library content. High-throughput analysis by flow cytometry makes it possible to interrogate vast numbers of probes or to perform large numbers of replicate measurements.

In suspension arrays, sets of beads carry a unique bar code.<sup>10,11</sup> To fully exploit the potential for multiplexed bead-based arrays, a robust and reliable method of manufacturing encoded beads is required. For high-throughput analysis, the decoding system must identify each and every code quickly and reliably. A number of encoding strategies have been proposed and demonstrated including the use of nanoscale metallic bar codes that are read by reflectance,<sup>12</sup> quantum dot-encoded mesoporous beads,<sup>13</sup> spatially resolved photobleaching of fluorescent particles,<sup>14</sup> direct optical reading of the shape of micromachined particles,<sup>15</sup> incorporation of Raman-active organic compounds,<sup>16</sup> or optical resonance (whispering gallery mode) in micrometer-sized silica spheres.<sup>17</sup>

\* To whom correspondence should be addressed. E-mail: hm@ecs.soton.ac.uk or plr2@soton.ac.uk.

<sup>†</sup> School of Chemistry, University of Southampton.

<sup>‡</sup> School of Electronics and Computer Science, University of Southampton.

<sup>§</sup> Optoelectronics Research Centre, University of Southampton.

<sup>||</sup> School of Physics and Astronomy, University of Southampton.

<sup>⊥</sup> Rutherford Appleton Laboratory.

(1) Gresham, D.; Ruderfer, D. M.; Pratt, S. C.; Schacherer, J.; Dunham, M. J.; Botstein, D.; Kruglyak, L. *Science* **2006**, *311*, 1932–1936.

(2) Abdullah-Sayani, A.; Bueno-de-Mesquita, J. M.; van de Vijver, M. J. *Nat. Clin. Pract. Oncol.* **2006**, *3*, 501–516.

(3) Becker, K. F.; Metzger, V.; Hipp, S.; Hofler, H. *Curr. Med. Chem.* **2006**, *13*, 1831–1837.

(4) Balboni, I.; Chan, S. M.; Kattah, M.; Tenenbaum, J. D.; Butte, A. J.; Utz, P. *J. Annu. Rev. Immunol.* **2006**, *24*, 391–418.

(5) Barbulovic-Nad, I.; Lucente, M.; Sun, Y.; Zhang, M. J.; Wheeler, A. R.; Bussmann, M. *Crit. Rev. Biotechnol.* **2006**, *26*, 237–259.

(6) Wingren, C.; Borrebaeck, C. A. K. *Omics* **2006**, *10*, 411–427.

(7) Bentley, D. R. *Curr. Opin. Genet. Dev.* **2006**, *16*, 545–552.

(8) Meza, M. B. *Drug Discovery Today* **2000**, 38–41.

(9) Nolan, J. P.; Mandy, F. *Cytometry, Part A* **2006**, *69A*, 318–325.

(10) Braeckmans, K.; De Smedt, S. C.; Leblans, M.; Pauwels, R.; Demeester, J. *Nat. Rev. Drug Discovery* **2002**, *1*, 447–456.

(11) Wilson, R.; Cossins, A. R.; Spiller, D. G. *Angew. Chem., Int. Ed.* **2006**, *45*, 6104–6117.

(12) Nicewarner-Pena, S. R.; Freeman, R. G.; Reiss, B. D.; He, L.; Pena, D. J.; Walton, I. D.; Cromer, R.; Keating, C. D.; Natan, M. J. *Science* **2001**, *294*, 137–141.

(13) Han, M. Y.; Gao, X. H.; Su, J. Z.; Nie, S. *Nat. Biotechnol.* **2001**, *19*, 631–635.

(14) Braeckmans, K.; De Smedt, S. C.; Roelant, C.; Leblans, M.; Pauwels, R.; Demeester, J. *Nat. Mater.* **2003**, *2*, 169–173.

(15) Zhi, Z. L.; Morita, Y.; Yamamura, S.; Tamiya, E. *Chem. Commun.* **2005**, 2448–2450.

(16) Jun, B. H.; Kim, J. H.; Park, H.; Kim, J. S.; Yu, K. N.; Lee, S. M.; Choi, H.; Kwak, S. Y.; Kim, Y. K.; Jeong, D. H.; Cho, M. H.; Lee, Y. S. *J. Comb. Chem.* **2007**, *9*, 237–244.

Nucleic acids have also been used as coding elements; these are read in situ by sequential hybridizations of labeled oligonucleotides<sup>18,19</sup> or via hybridization to a conventional DNA chip after removal of the tag sequence from the beads.<sup>20</sup>

Among these, spectral encoding, based on fluorescence wavelength and intensity, appears to be the most promising. However, this approach limits the number of bead-based assays that can be performed to the number of spectrally resolvable fluorophores that can be incorporated into a bead. Current spectral encoding technology (e.g., Luminex xMAP) provides ~100 unique codes. In principle, the possibilities are far greater; for example, 6 colors at 10 intensity levels gives ~1 million codes. However, practical encoding capabilities are much lower (due to spectral overlap, fluorescence intensity variations, signal-to-noise ratio, etc.) and realistically five to six colors with six intensity levels could yield ~10 000–40 000 codes.<sup>10</sup> A major drawback of this method is that most bead-based biochemical assays rely on fluorescence readout, so that the additional use of fluorescence for encoding, particularly where multiple fluorophores are used, places limits on the spectral bandwidth available for fluorescent-based assays or the number of individual codes that can be identified. Recently, a method for fabricating graphical bar codes within microfluidic channels was reported. Using laminar flow, separate coding and probing regions were simultaneously assembled during a polymerization step.<sup>21</sup> The potential for encoding ~10<sup>6</sup> unique codes in particles of length 180–270  $\mu\text{m}$  was demonstrated.

We have developed a new and robust encoding system, orthogonal to fluorescence-based assays, based on microparticles that incorporate diffractive elements as identifiers.<sup>22</sup> Noninvasive and noncontact reading of codes can be accomplished by analyzing the spatial distribution of the diffracted light. This is shown schematically in Figure 1, which demonstrates the principle of encoding using microdiffraction gratings. A single grating diffracts the incident light into a unique diffraction pattern as shown in Figure 1a. The “code” is read by measuring the spatial distribution of this diffracted light. In the simplest implementation, information is encoded in the pitch of the grating,  $a$ . When the grating is illuminated with light at wavelength  $\lambda$ , a series of diffracted beams is created at angles  $\theta$ , according to eq 1, where  $m$  is the order of the diffracted beam. Measurement of the first order ( $m = \pm 1$ ) diffracted beam position (with respect to the zero order) gives direct information about the pitch  $a$ . This is shown in Figure 1a and b.

$$a \sin \theta = m\lambda \quad (1)$$

We have previously demonstrated that ~10<sup>9</sup> unique codes can be created from a library of five times superimposed gratings fabricated on a 100- $\mu\text{m}$ -long particle.<sup>22</sup> In fact, the encoding has recently been extended to two dimensions, greatly amplifying the

encoding capacity to huge numbers; up to 10<sup>18</sup> unique codes.<sup>23</sup> Shrinking the gratings reduces the encoding capacity; the value quoted above is for a 100- $\mu\text{m}$  particle read with a laser light of wavelength 633 nm. The lower limit of grating size is ~3 times the wavelength of the reading laser (in our case, ~1.9  $\mu\text{m}$ ); however, gratings of this size only have one possible code. The encoding capacity increases rapidly as the grating size is increased, already reaching ~10<sup>4</sup> codes for 10- $\mu\text{m}$  gratings.

In this paper, we assess the functionality of probe biomolecules immobilized onto these diffractive micro bar codes, namely, immunoglobulin Gs (IgGs) and DNA. We characterize the thermodynamics and kinetics of their molecular interactions and go on to demonstrate their use in multiplexed assays.

## EXPERIMENTAL SECTION

**Optical Hardware.** Simultaneous diffraction and fluorescence measurements were made using a custom-made optical system with an infinity corrected high numerical aperture objective lens and appropriate optical band-pass filters and dichroics (Supporting Information Figure S-2). Diffraction patterns were generated using plane incident light. The diffracted light was collected by a CCD camera and the diffraction pattern analyzed by dedicated computer software.

**Particle Fabrication.** Diffractive bar codes were fabricated from photoactive epoxy SU-8-5 (Chestech Ltd. Rugby, UK). The resist was spin-coated onto Si wafers (525  $\pm$  25  $\mu\text{m}$  thick) onto which a thin layer of Al had been evaporated. After spinning onto the primed wafers, the SU-8 was soft baked, exposed (using an EVG 620 mask aligner with photomask from Compugraphic, UK), and postexposure baked. The wafers were then developed in EC solvent poly(propylene glycol) methyl ether acetate (Chestech Ltd., Rugby, UK) for 2 min with agitation. The wafers were thoroughly rinsed with isopropyl alcohol and blow dried. The Al sacrificial layer was removed by sonicating the wafers in Microposit MF-319 (tetramethylammonium hydroxide (2.2% w/v solution in water), Chestech Ltd., Rugby, UK) at room temperature for 10 min. The microparticles were collected by centrifugation (12500g, 1 min), washed in methanol (1 mL  $\times$  8), and dried under vacuum at room temperature for 4 h.

**Reagents.** Oligonucleotides (P1, 5'-biotin-AAAAAGTTGGATCC-3'; P2, 5'-biotin-AAAACTTGGATCC-3'; C1, 5'-Cy5-GGGATC-CAAGTTTTT-3'; FP1, 5'-Cy5-CTAGTTACTCTTGTTC-biotin-3') were purchased from ATDBio (Southampton, UK) or synthesized using a MerMade 192 DNA synthesizer (Bioautomation Inc.), for which all reagents were obtained from Link Technologies (Bellshill, UK). Cy3-labeled goat polyclonal anti-human IgG and Cy5-labeled goat polyclonal anti-rabbit IgG, anti-mouse IgG, and anti-guinea pig IgG were purchased from Abcam plc. (Cambridge, UK).

**Conjugation of Oligonucleotides and IgGs to Encoded Microparticles.** SU-8 microparticles for use in both hybridization assays and immunoassays were functionalized by reaction of avidin-DN (Vector laboratories, Burlingame, CA) or protein A (Cambridge Bioscience, Cambridge, UK), respectively, with carboxyl-functionalized particles according to standard amide coupling protocols.<sup>24</sup> Carboxyl groups were introduced by succinylation of primary amine groups resulting from ring opening of

(17) Vollmer, F.; Arnold, S.; Braun, D.; Teraoka, I.; Libchaber, A. *Biophys. J.* **2003**, *84*, 295A–295A.

(18) Gunderson, K. L.; Kruglyak, S.; Graige, M. S.; Garcia, F.; Kermani, B. G.; Zhao, C. F.; Che, D. P.; Dickinson, T.; Wickham, E.; Bierle, J.; Doucet, D.; Milewski, M.; Yang, R.; Siegmund, C.; Haas, J.; Zhou, L. X.; Oliphant, A.; Fan, J. B.; Barnard, S.; Chee, M. S. *Genome Res.* **2004**, *14*, 870–877.

(19) Li, Y. G.; Cu, Y. T. H.; Luo, D. *Nat. Biotechnol.* **2005**, *23*, 885–889.

(20) Nam, J. M.; Thaxton, C. S.; Mirkin, C. A. *Science* **2003**, *301*, 1884–1886.

(21) Pregibon, D. C.; Toner, M.; Doyle, P. S. *Science* **2007**, *315*, 1393–1396.

(22) Galitonov, G. S.; Birtwell, S. W.; Zheludev, N. I.; Morgan, H. *Opt. Express* **2006**, *14*, 1382–1387.

(23) Birtwell, S. W.; Galitonov, G. S.; Morgan, H.; Zheludev, N. I. *Opt. Commun.* In press. Doi:10.1016/j.optcom.2007.04.066.

(24) Hermanson, G. T. *Bioconjugate Techniques*; Academic Press: London, 1996.

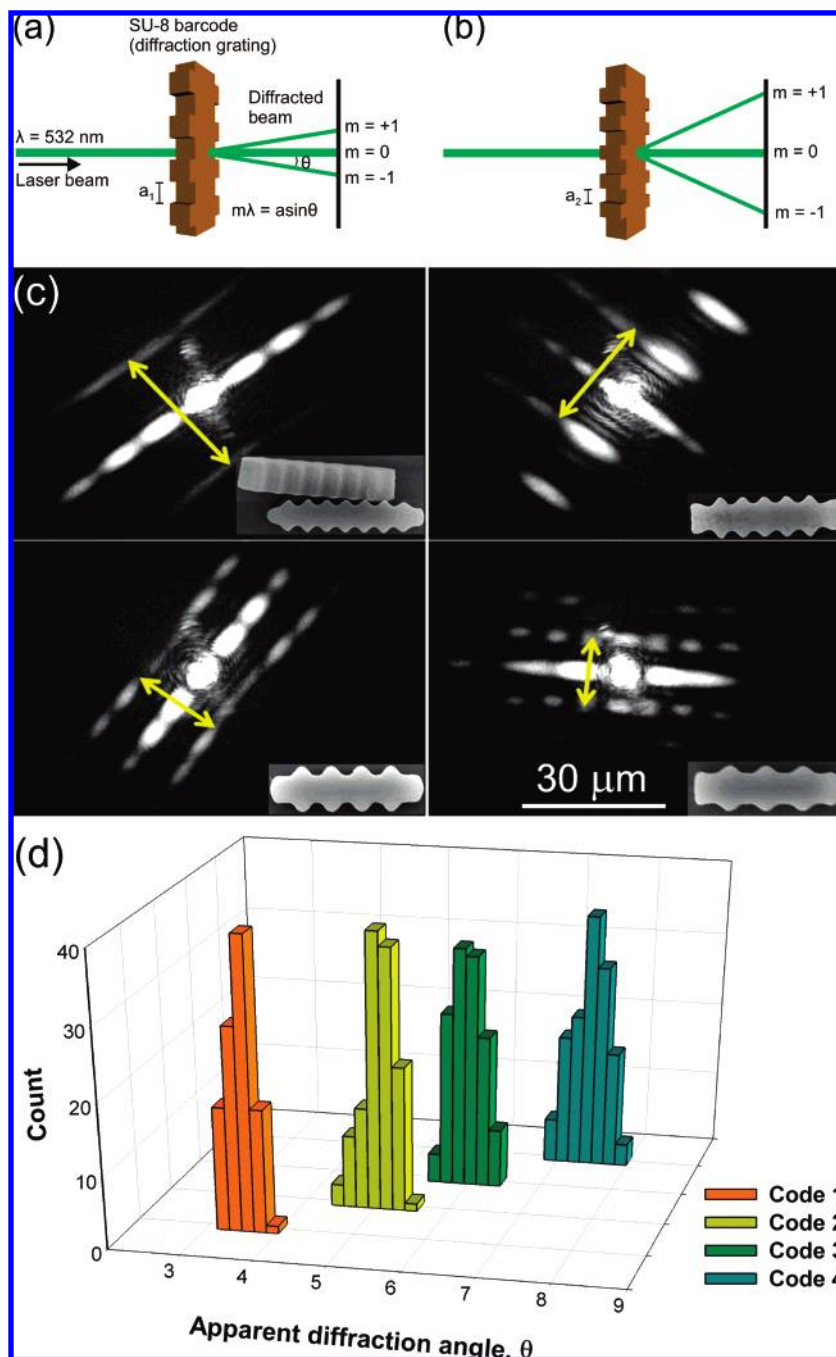


**Figure 1.** (a) First-order ( $m = \pm 1$ ) diffraction from a grating with pitch  $a_1$ . (b) First-order diffraction from a grating with pitch  $a_2$ , where  $a_1 > a_2$ . The two codes are distinguishable if the beam separation is greater than the beam width. (c) Four different SU-8 microparticles with their corresponding diffraction patterns immersed in water. Insets show micrographs of the particles manufactured by optical lithography. The separations between the first-order diffraction lines, which vary with the inverse of the grating period, are indicated. (d) Histogram showing the distribution of observed diffraction angles from particles used in multiplexed assays.

residual surface epoxide groups of SU-8 with Jeffamine, as described previously.<sup>25</sup> Detailed protocols for all synthetic steps are available as Supporting Information.

#### Determination of Equilibrium Dissociation Constants.

Thermodynamics of molecular interactions were determined using titration of analytes and flow cytometry. Human IgG-coated SU-8 microparticles (1 mg), suspended in storage buffer (10 mM  $\text{NaH}_2\text{PO}_4$ , 150 mM NaCl, 0.1% Tween-20, pH 7.8, 100  $\mu\text{L}$ , giving a 0.75

$\mu\text{M}$  concentration of immobilized human IgG) were incubated with Cy5-labeled detector antibody (3 pM) at room temperature for 15–30 min. An aliquot of the sample (5  $\mu\text{L}$ ) was withdrawn, immediately washed with PBS (200  $\mu\text{L}$ ), and stored at 4  $^\circ\text{C}$  in the dark. The microparticles were separated from the reaction mixture by centrifugation (12500g, 1 min), and an aliquot of the supernatant (5  $\mu\text{L}$ ) was removed. A further aliquot of Cy5-labeled anti-IgG was added, and the above procedures were repeated. The fluorescence intensity of the samples was measured by fluorescence-activated cytometry.

(25) Cavalli, G.; Banu, S.; Ranasinghe, R. T.; Broder, G. R.; Martins, H. F. P.; Neylon, C.; Morgan, H.; Roach, P. L. *J. Comb. Chem.* **2007**, 462–472.



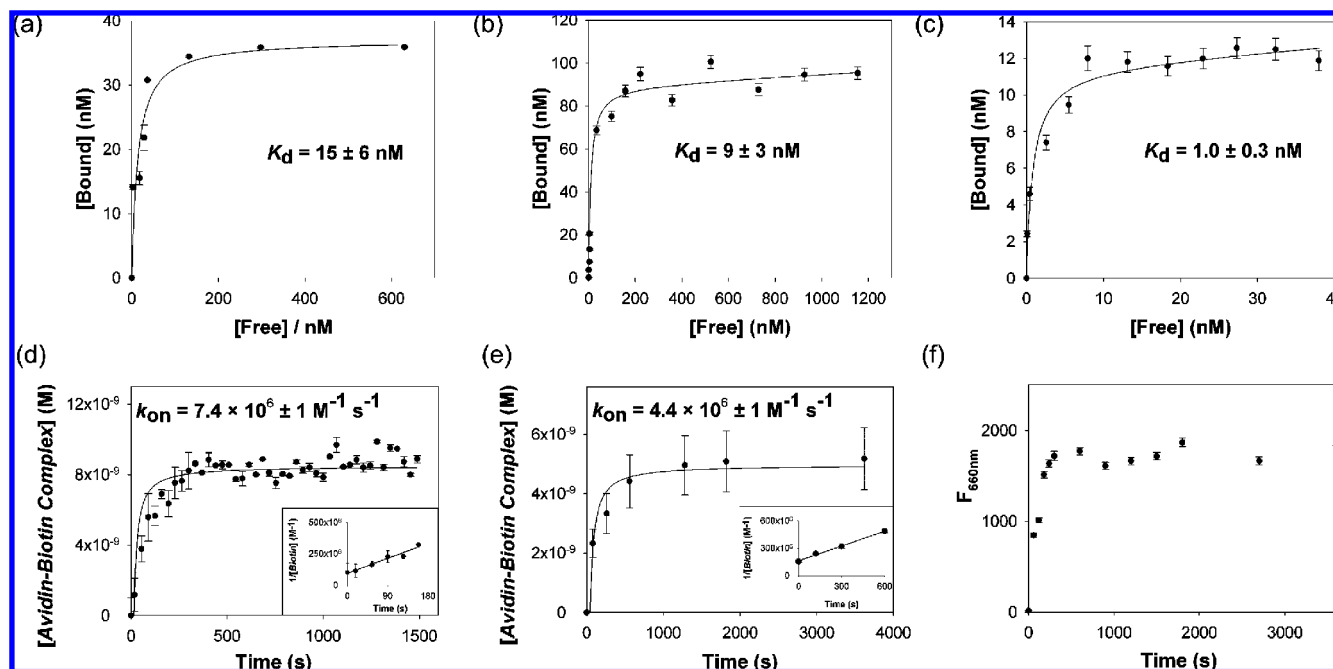


**Figure 2.** Saturation binding curves for Cy5-anti human IgG interaction in solution (a) on SU-8 microparticles, (b) and for avidin-DN/Cy5-labeled biotinylated oligonucleotide FP1 on SU-8 particles (c). Time-course measurements of avidin/biotin binding in solution (d) and with avidin-DN immobilized on SU-8 microparticles (e), with insets showing linear plots of the integrated rate equation. Panel f shows fluorescence time-course measurement of human IgG/anti-human IgG binding on encoded microparticles.

Solution-phase data for the human IgG/anti-human IgG interaction were obtained by measuring fluorescence polarization. To a solution of Cy5-labeled goat anti-human IgG (0.67 nM) in buffer (10 mM  $\text{NaH}_2\text{PO}_4$ , 150 mM NaCl, 0.01%  $\text{NaN}_3$ , pH 7.8) was added human-IgG (final concentration 0–666 nM), and the reaction mixture was incubated at room temperature in the dark for 16 h. The fluorescence polarization of each of the samples was recorded using a microplate reader (Safire<sup>2</sup>, Tecan, Switzerland,  $\lambda_{\text{ex}} = 635$  nm,  $\lambda_{\text{em}} = 666$  nm).

Avidin-DN coated SU-8 microparticles (0.4 mg), suspended in SSPE (5 $\times$ ) buffer (0.75 M NaCl, 50 mM  $\text{NaH}_2\text{PO}_4$ , 5 mM EDTA, 0.02% Tween-20, pH 7.0, 250  $\mu\text{L}$ , giving a 0.1  $\mu\text{M}$  concentration of immobilized avidin-DN), were incubated with Cy5-labeled biotinylated oligonucleotide, FP1 (2.5 nM) at room temperature for 15–30 min. An aliquot of the sample (10  $\mu\text{L}$ ) was withdrawn and stored at 4  $^\circ\text{C}$  in the dark. The microparticles were separated from the reaction mixture by centrifugation (12500g, 1 min), and an aliquot of the supernatant (5  $\mu\text{L}$ ) was removed. A further aliquot of FP1 was added, and the above procedures were repeated. The fluorescence intensity of the samples was measured by fluorescence-activated flow cytometry (FACS).

The data (Figure 2) were fitted to a ligand-binding function (eq 2, where [Bound], [Free], and [Nonspecific] refer to concentrations of specifically bound, free, and nonspecifically bound Cy5-labeled analyte) using commercially available software (SigmaPlot 9, Systat Inc., San Jose, CA), to determine the total number of binding sites ( $B_{\text{max}}$ ) and  $K_d$ .

$$[\text{Bound}] = \frac{B_{\text{max}}[\text{Free}]}{K_d + [\text{Free}]} + [\text{Nonspecific}][\text{Free}] \quad (2)$$

**Kinetic Analysis of Avidin/Biotin Binding.** Avidin-coated SU-8 microparticles, (0.08 mg, bearing 5.7 pmol of avidin-DN) were

suspended in SSPE (5 $\times$ ) buffer (45.5  $\mu\text{L}$ ). Biotinylated Cy-5 labeled oligonucleotide (FP1) was added (0.3 nmol, final concentration 6.5 nM). The suspension was agitated and aliquots (5  $\mu\text{L}$ ) were removed periodically for immediate analysis, without washing. The fluorescence intensity of the samples was measured by fluorescence-activated cytometry.

Solution-phase data were obtained by measuring fluorescence polarization. A solution containing biotinylated Cy-5-labeled oligonucleotide (FP1, 0.2 pmol, final concentration 1 nM), biotin (1.8 pmol, final concentration 9 nM), and avidin-DN (2 pmol, final concentration 10 nM) in SSPE (5 $\times$ ) buffer (200  $\mu\text{L}$ ) was incubated at room temperature. (Note: Solutions containing only FP1 and avidin-DN were found to undergo self-quenching upon binding, presumably due to the proximity of four fluorophores to each other in the protein tetramer.) The fluorescence polarization was recorded periodically using a microplate reader (Safire<sup>2</sup>, Tecan, Switzerland,  $\lambda_{\text{ex}} = 635$  nm,  $\lambda_{\text{em}} = 666$  nm).

Both data sets were fitted to eq 3 using commercially available software (SigmaPlot 9, Systat Inc., San Jose, CA) in order to determine the rate constant,  $k_{\text{on}}$ .

$$\frac{\partial[\text{Avidin} - \text{Biotin Complex}]}{\partial t} = k_{\text{on}}[\text{Free Avidin}][\text{Free Biotin}] \quad (3)$$

**Kinetic Analysis of Human IgG/Anti-Human IgG Binding on Encoded Microparticles.** Human IgG immobilized SU-8 microparticles (1 mg), suspended in storage buffer (100  $\mu\text{L}$ ), were incubated with Cy5-labeled detector antibody (6.67 pmol, final concentration 67 nM) at room temperature. After fixed time intervals, samples (5  $\mu\text{L}$ ) were withdrawn, immediately washed with storage buffer (200  $\mu\text{L}$ ), and stored at 4  $^\circ\text{C}$  in the dark. The

fluorescence intensity of the samples was measured by fluorescence-activated cytometry.

**Multiplexed DNA Hybridization Assay.** Biotinylated oligonucleotides P1 and P2 were captured onto encoded particles by immobilized avidin in 5× SSPE buffer in separate reactions. A mixture of the encoded particles underwent hybridization to C1 (1 pmol, 3 nM) in 5× SSPE buffer at room temperature for 40 min, followed by centrifugation and resuspension in 2 M aqueous urea for 2 min. The microparticles were then washed twice with 5× SSPE buffer before analysis.

**Multiplexed Immunoassays.** Polyclonal IgGs from human, rabbit, guinea pig, or mouse IgG were captured onto encoded particles by immobilized protein A in PBS in separate reactions. Labeled anti-IgGs (Cy3- or Cy5-labeled, supplied by Abcam, Cambridge, UK, 13 pmol, 260 nM) were added to the appropriate mixture of the encoded particles in PBS at room temperature for 1 h, with occasional gentle agitation. The microparticles were then washed twice with PBS before analysis.

**Statistical Analysis of Fluorescence Measurements and Estimate of Sensitivity of Multiplexed Assays.** Student's *t*-test was used to calculate values of *P* for measured fluorescence intensities for positive and negative data sets (using Microsoft Excel). The sensitivity of assay for anti-human IgG was estimated according to  $K_d$ ,  $B_{\max}$ , and the number of required replicate measurements as follows. The ratio of complexed to free protein concentration is determined through eq 4:

$$[\text{Free Analyte}] = K_d[\text{Complex}]/[\text{Free Probe}] \quad (4)$$

Assuming 20 particles are measured ( $P < 0.0003$  for all data sets measured), then  $[\text{Free Probe}] + [\text{Complex}] = 0.37 \text{ nM}$ , and at saturation  $[\text{Complex}] = 0.37 \text{ nM}$ . Hence  $[\text{Complex}]$  required for a signal/noise ratio of five =  $(5 \div 7.7) \times 0.37 \text{ nM} = 0.24 \text{ nM}$ , and  $[\text{Free Probe}] = 0.37 \text{ nM} - 0.24 \text{ nM} = 0.13 \text{ nM}$ . Substituting into eq 4 gives  $[\text{Free Analyte}] = 16.6 \text{ nM}$ . Therefore, the total concentration of analyte in the sample =  $[\text{Free Analyte}] + [\text{Complex}] = 16.6 + 0.37 = 16.97 \text{ nM}$ .

## RESULTS AND DISCUSSION

**Particle Fabrication.** The multiplexed encoding principle was demonstrated using bar-shaped microparticles fabricated using conventional photolithography from a photoactive epoxy resin (SU-8).<sup>26</sup> This material has been previously shown to be suitable for multistep solid-phase peptide and oligonucleotide synthesis.<sup>25</sup> Micrometer-sized diffraction gratings were created using particles with serrated edges, as shown in Figure 1c. The advantage of this method is that it involves a single photolithographic step. Large numbers of particles ( $2.5 \times 10^6$  particles/silicon wafer) can be manufactured with identical chemical and physical properties using this method. More complex and higher density gratings can be made by nanoembossing.<sup>26,27</sup> The diffracted first-order beams from the four codes used for multiplexed assays are sufficiently separated in angular space to permit unambiguous decoding, with a small overlap between codes 2 and 3 (Figure 1d). Data from particles with diffraction angles within the overlap region were discarded.

**Thermodynamic and Kinetic Characterization of Probes Attached to Encoded Microparticles.** One of the advantages of particle-based suspension arrays over planar array formats is that reaction kinetics and thermodynamics resemble those observed in solution phase, enabling higher throughput and sensitivity.<sup>28</sup> In order to demonstrate these principles, we measured binding thermodynamics and kinetics on our encoded microparticles via titrations of analyte binding and fluorescence time-course experiments.

We determined the equilibrium dissociation constants for key molecular interactions by carrying out binding titrations (Figure 2a–c). These data confirm that both anti-IgG/IgG ( $K_d$  in solution =  $15 \pm 6 \text{ nM}$ ;  $K_d$  on SU-8 microparticles =  $9 \pm 3 \text{ nM}$ ) and avidin/biotin ( $K_d$  in solution =  $1 \times 10^{-6} \text{ nM}$ ;<sup>29</sup>  $K_d$  on SU-8 microparticles =  $1 \pm 0.3 \text{ nM}$ ) interactions retained high affinity when transferred to the solid phase, though in the case of avidin/biotin, a significant reduction in affinity was observed, which may be due to the use of recombinant avidin-DN or the bulky oligonucleotide–biotin conjugate. From  $B_{\max}$ , the number of analyte molecules bound to each microparticle at saturation was calculated. For Cy5-labeled anti-IgG, this value was  $\sim 10^7$  molecules (or 17 amol) per particle, while  $\sim 0.8 \times 10^7$  molecules (or 13 amol) of Cy5-labeled biotinylated oligonucleotide were bound to each microparticle.

The kinetics of binding of Cy5-labeled biotinylated oligonucleotide to immobilized avidin-DN, and Cy5-labeled anti-human IgG to human IgG were analyzed by carrying out fluorescence time-course experiments. For the avidin-DN-biotinylated oligonucleotide interaction (Figure 2d), the data were fitted to eq 3 in order to calculate  $k_{\text{on}}$ , with the linear plots of the integrated rate equation used to confirm the second-order nature of the reaction. The value obtained on SU-8 particles ( $4.4 \times 10^6 \text{ M}^{-1} \text{ s}^{-1}$ ) was very close to that observed in solution for avidin-DN/biotinylated oligonucleotide FP1 ( $7.4 \times 10^6 \text{ M}^{-1} \text{ s}^{-1}$ ) and within the range previously reported for the native biotin–avidin interaction ( $k_{\text{on}} = 5 \times 10^5 - 8.2 \times 10^7 \text{ M}^{-1} \text{ s}^{-1}$ ).<sup>29</sup> For the kinetically more complex sandwich system used for binding of labeled detection IgGs, we did not attempt to parse individual rate constants but simply measured the time taken for a system containing a 67 nM concentration of analyte to reach equilibrium (Figure 2f), which was found to be <10 min. We were therefore able to confirm that binding assays on our encoded microparticles can be carried out in short time scales.

**Multiplexed Biomolecular Assays.** Multiplexed analysis was demonstrated using the four different photolithographically fabricated bar codes (designated codes 1–4) shown in Figure 1c. These codes can easily be differentiated with the aid of a light microscope, but to increase throughput, the bar codes were read using an automated recognition and analysis system that captured the diffraction image on a CCD camera. Image processing software identifies a particle from the captured image, assigns a direction vector to the principal axis, and then performs a Fourier analysis of the first-order spots to determine the particle code. This process is performed at high speed, taking less than 1 ms.

A multiplexed DNA hybridization assay was performed using sequences corresponding to a polymorphic locus (N1303K) on the gene encoding the cystic fibrosis transmembrane conductance

(26) Banu, S.; Birtwell, S. W.; Galitonov, G. S.; Chen, Y.-F.; Zheludev, N. I.; Morgan, H. J. *Micromech. Microeng.* **2007**, *17*, S116–S121.

(27) Guo, L. J. *J. Phys. D* **2004**, *37*, R123–R141.

(28) Finkel, N. H.; Lou, X.; Wang, C.; He, L. *Anal. Chem.* **2004**, *76*, 352A–359A.

(29) Green, N. M. *Biochem. J.* **1963**, *89*, 585.

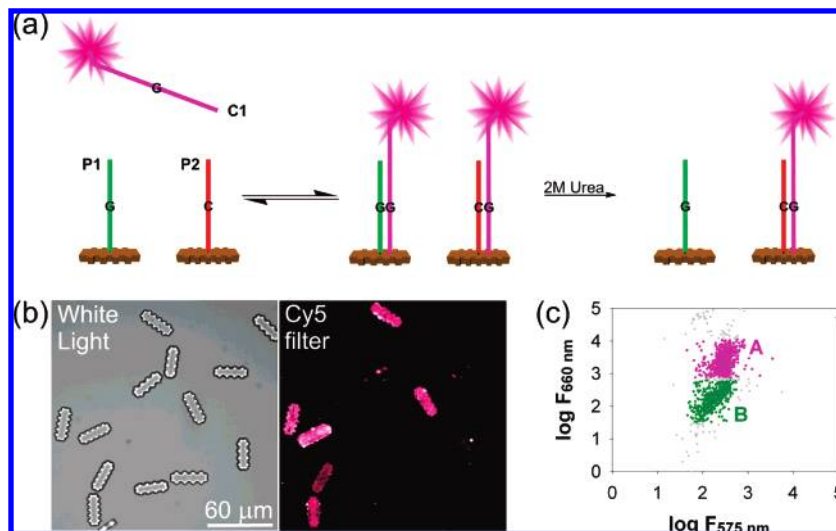


**Figure 3.** Assay used to differentiate oligonucleotides differing by a single nucleotide. (a) Two different oligonucleotides (P1 and P2) that vary only at a single position are bound to encoded microparticles. After hybridization to a third oligonucleotide (C1) that is a perfect match for one sequence, the particles were washed in 2 M urea and then imaged. (b) White light microscope image (left panel) and fluorescence image (right panel). The particles bearing the perfectly matched sequence fluoresce and those with the single mismatch do not. (c) Scatter plot of the two populations (A and B). These were sorted by FACS on the basis of Cy5 fluorescence and the codes of 50 particles in each population read.

regulator protein (Figure 3a).<sup>30</sup> Two sets of encoded particles were functionalized with avidin and used to capture biotinylated probe oligonucleotides. Wild type sequence P2 was bound to code 3 and the mutant sequence, P1, differing by a single nucleotide, was attached to code 2. Figure 3b shows a microscope image and fluorescence image of the two particle types, demonstrating that the perfectly matched sequence hybridizes but the mismatched sequence does not. The observed fluorescence shows a degree of inhomogeneity across the particle although the physical basis for this observation has not yet been determined. The particles were assayed using conventional flow cytometry, and the scatter plot for the two different populations is shown in Figure 3c. Sorting on the basis of the fluorescence signal, followed by decoding of a representative sample of particles (50 from each fraction) showed that the hybridized population consisted of 96% code 3, with the unhybridized population B consisting of 96% code 2. These results demonstrate that the use of diffractively encoded microparticles permits discrimination of a single mismatch from a Watson–Crick base pair within a short DNA duplex, confirming their applicability to SNP genotyping applications.

To demonstrate the applicability of the technology to immunodiagnosics, a multiplexed immunoassay was implemented for the detection of IgGs. Two sets of encoded particles were functionalized with two different IgGs using protein A capture. The particles were incubated with complementary antibodies as shown schematically in Figure 4a. The fluorescence images (Figure 4b) show the selective binding of the differentially labeled

detection antibodies to the correct encoded particle. The labeled particles were again analyzed using flow cytometry and sorted into two populations on the basis of relative fluorescence (Figure 4c). A total of 50 particles from each of these two sorted populations were then decoded, showing that particles from the Cy5-labeled population (A) were correctly identified as code 2, and the Cy3-labeled population (B) as code 4 with greater than 95% accuracy.

A prerequisite for reliable multiplexed immunoassays is the demonstration of selective antigen–antibody binding against a background of other potentially competing interactions. Therefore, a small library consisting of four sets of different encoded particles were each functionalized with a different antigen. Mixtures of fluorescently labeled detection antibodies were added to aliquots of the library (Figure 4d). For the experiments described above, a two-step sorting/decoding process was used to read the code and measure the fluorescence from each particle. Since this approach is not amenable to high-throughput analysis, the microparticles from these quadruplexed experiments were dispersed on a microscope slide and analyzed using a modified optical microscope setup capable of reading diffraction and fluorescence intensity. Manual reading of each particle using this apparatus took ~10–30 s. Binding of the complementary antibody gave fluorescence intensities in the range 250 000–430 000 (au, corrected for the quantum yield of the detection antibodies). Control particles, whose corresponding anti-IgG was not present in the sample, had intensities in the range 13 000–58 000 (au), demonstrating very little cross-reaction.

**Replicate Measurements within Multiplexed Assays and Analyte Sensitivity.** The throughput and sensitivity of microparticle-based assays is determined in practice by the detectable amount of analyte per particle and the number of replicate samples that must be measured to satisfy a set confidence level in the results. The latter in turn is determined by the variation of signal (in this case fluorescence) between particles of the same type that have been subject to the same assay conditions. We analyzed data

(30) Osborne, L.; Santis, G.; Schwarz, M.; Klinger, K.; Dork, T.; McIntosh, I.; Schwartz, M.; Nunes, V.; Macek, M.; Reiss, J.; Highsmith, W. E.; McMahon, R.; Novelli, G.; Malik, N.; Burger, J.; Anvret, M.; Wallace, A.; Williams, C.; Mathew, C.; Rozen, R.; Graham, C.; Gasparini, P.; Bal, J.; Cassiman, J. J.; Balassopoulou, A.; Davidow, L.; Raskin, S.; Kalaydjieva, L.; Kerem, B.; Richards, S.; Simonbouy, B.; Super, M.; Wulbrand, U.; Keston, M.; Estivill, X.; Vavrova, V.; Friedman, K. J.; Barton, D.; Dallapiccola, B.; Stuhmann, M.; Beards, F.; Hill, A. J. M.; Pignatti, P. F.; Cuppens, H.; Angelicheva, D.; Tummler, B.; Brock, D. J. H.; Casals, T.; Macek, M.; Schmidtke, J.; Magee, A. C.; Bonizzato, A.; Deboeck, C.; Kuffardjieva, A.; Hodson, M.; Knight, R. A. *Hum. Genet.* **1992**, *89*, 653–658.



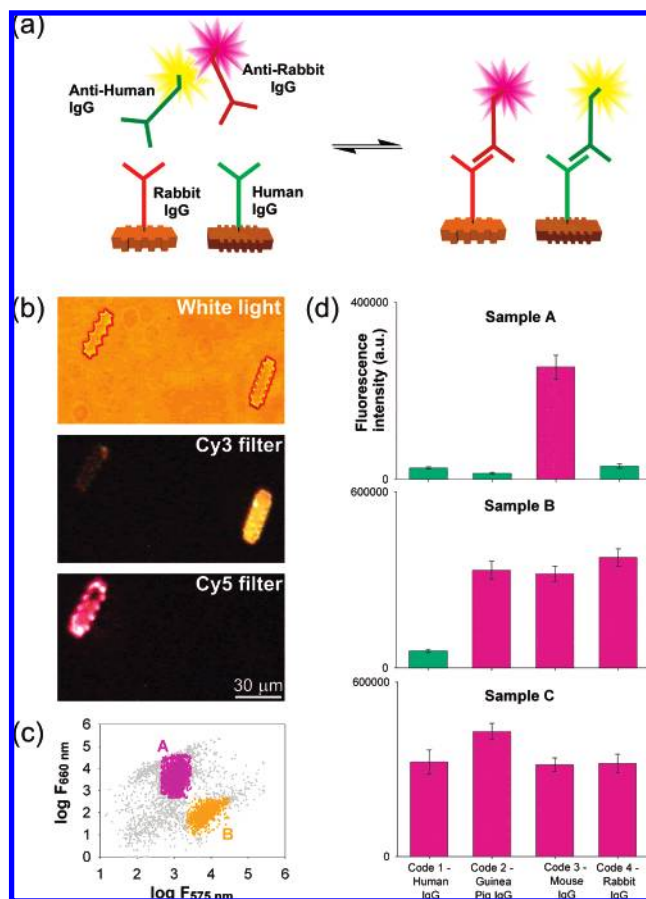


**Figure 4.** Multiplexed immunoassays with encoded microparticles. (a) Rabbit and human antibodies are attached to encoded microparticles, which are then mixed with detection antibodies in a single reaction. Detection antibodies were Cy3-labeled anti-human and Cy5-labeled anti-rabbit IgG, respectively. (b) Microscope images of two particles from the multiplex reaction, imaged with white light (top), Cy3 fluorescence (middle) and Cy5 fluorescence (bottom). The faint fluorescence from code 2 in the second image (Cy3 filter) is due to the intrinsic fluorescence of the SU-8 polymer<sup>34</sup> and not to cross-reaction of the Cy3-labeled antibody. (c) Scatter plot for two populations of particles, which were then sorted on the basis of Cy3 and Cy5 fluorescence and the codes of 50 particles in each population read. Population A: (bar code 2, 49 (98%); bar code 4, 0 (0%); unreadable/incorrectly identified, 1 (2%). Population B: (bar code 2, 0 (0%); bar code 4, 50 (100%); unreadable/incorrectly identified, 0 (0%). (d) Results from the quadruplex immunoassay showing mean particle fluorescence intensity ( $n = 15\text{--}25$ ) for a small library of four different IgG functionalized bar codes after addition of Cy5-labeled anti-IgGs to an aliquot of the library. Sample A: only anti-mouse IgG was added, binding selectively to code 3. The mean fluorescence following binding (and washing) of  $\sim 100$  particles is shown (with standard error). Sample B: anti-guinea pig, anti-mouse, and anti-rabbit IgG were all added to an aliquot of the codes, giving a fluorescent "readout" as for sample A. Sample C: all four complementary fluorescently labeled antibodies were added to the sample of four codes.

from the quadruplex immunoassay and single base mismatch DNA hybridization assay, since these assays are the most complex and have the highest probability of cross-reactions and high background fluorescence, allowing the most realistic estimation of these parameters. Mean fluorescence intensities with standard deviations for representative positive (complementary anti-IgG or oligonucleotide present) and negative (complementary anti-IgG

or oligonucleotide absent) data sets are shown in Figure 5a and c. Though the standard deviations of positive and negative populations are well separated, the coefficients of variance (47–60%) are larger than those typical of optimized ELISAs (5–10%).<sup>31</sup> A possible contribution to these relatively large coefficients of variance may be the observed inhomogeneity of the fluorescence (Figures 3b and 4b). There is therefore a nonzero probability of any given particle within either positive or negative population giving a fluorescent signal that falls within the range attributed to the other population, i.e., generating a false positive or false negative signal.

Student's  $t$ -test was used to compare the difference between "negative" and "positive" data sets from the quadruplex immunoassay and DNA hybridization assay. Cumulative  $P$  values from three positive data sets are plotted against number of particles read, Figure 5b and d. As expected, as more particles are read, the value of  $P$  falls, indicating greater confidence in the difference between data sets. After reading 11 particles, the probability of any of the positive data sets being indistinguishable from the negative data set is  $<0.01$ , and after reading 16 particles, the probability is  $<0.0003$ . Therefore, for multiplexed platforms where thousands of molecular interactions are assayed, measurement of 15–20 replicates is necessary to satisfy a confidence level of  $>99.97\%$ . This level of degeneracy is greater than that necessary for ELISAs, but is comparable to that used in Illumina BeadArrays where  $\sim 30$  replicate beads are used for each oligonucleotide to enable averaging and thorough statistical analysis of results.<sup>32</sup> From  $B_{\max}$ , the number of analyte molecules bound to each microparticle at saturation can be calculated. For Cy5-labeled anti-IgG, this was  $\sim 10^7$  molecules (or 17 amol) per particle; a similar number ( $\sim 0.8 \times 10^7$  molecules, or 13 amol) of Cy5-labeled biotinylated oligonucleotide were bound to each microparticle. Given the number of replicate particles required for analysis, we can estimate the amount of bound analyte required to generate a positive signal. The maximum binding capacity of a single particle is  $\sim 10^7$  molecules (17 amol); therefore, 20 particles will be saturated by 340 amol of bound (labeled) IgG or DNA analyte. The sensitivity of individual assays will be determined by the signal/noise ratio (SNR) obtained for the analyte and its affinity for the immobilized complementary probe. For example, Figure 5a shows that the human IgG/anti-human IgG interaction, has a SNR (at saturation) of 7.7, with  $K_d = 9 \pm 3$  nM. Assuming that a SNR of 5 is sufficient for detection, and that the assay is carried out in a volume of  $1 \mu\text{L}$ , eq 4 can be used to determine the total concentration of anti-human IgG required to produce a signal. This predicts that the total concentration of analyte in the sample is 16.97 nM, giving an estimate of sensitivity of approximately 17 fmol, or  $10^{10}$  molecules. This is a relatively conservative estimate of sensitivity; if a cutoff value equal to twice background fluorescence is used, as for other bead-based assays,<sup>33</sup> the sensitivity increases to a detection limit of 5.35 fmol (in a  $1\text{-}\mu\text{L}$  volume), or  $3.2 \times 10^9$  molecules. To demonstrate this experimentally, we

(31) de Jager, W.; Rijkers, G. T. *Methods* **2006**, *38*, 294–303.

(32) Novak, J. P.; Miller, M. C.; Bell, D. A. *Biol. Direct* In press. DOI 10.1186/1745-6150-1-18.

(33) Dunbar, S. A.; Vander Zee, C. A.; Oliver, K. G.; Karem, K. L.; Jacobson, J. W. *J. Microbiol. Methods* **2003**, *53*, 245–252.

(34) Marie, R.; Schmid, S.; Johansson, A.; Ejsing, L. E.; Nordstrom, M.; Hafziger, D.; Christensen, C. B. V.; Boisen, A.; Dufva, M. *Biosens. Bioelectron.* **2006**, *21*, 1327–1332.



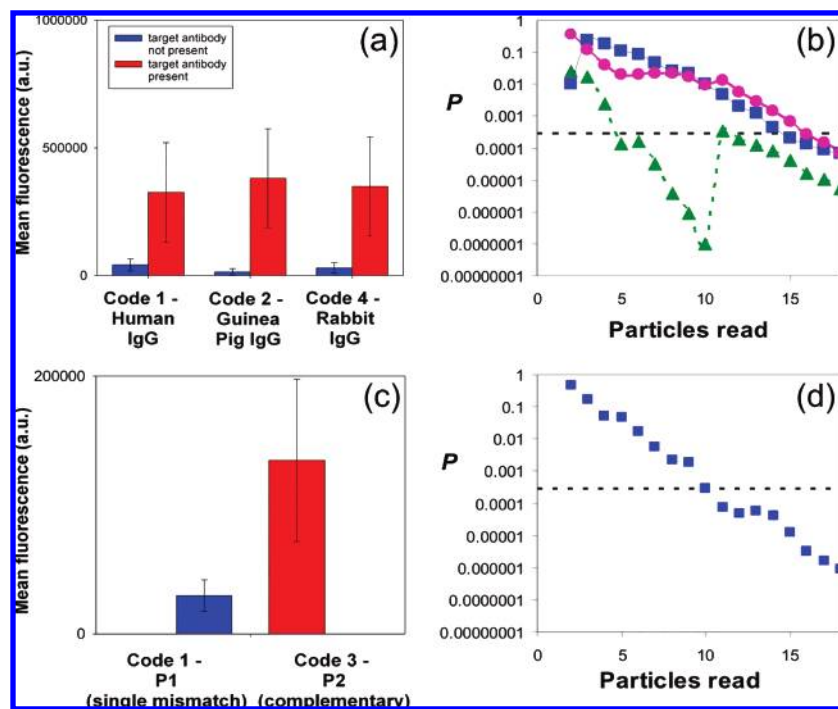


**Figure 5.** Mean fluorescence intensities with standard deviations for representative positive (complementary anti-IgG or labeled oligonucleotide present) and negative (complementary anti-IgG or labeled oligonucleotide absent) particle sets functionalized with different probes, (a) and (c), and cumulative  $P$  values from positive data sets plotted against read number, (b) and (d). Data from particles functionalized with human IgG (blue squares), guinea pig IgG (green triangles), and rabbit IgG (pink circles) are compared in (b), while data from P2- and P1-functionalized particles (differing by a single nucleotide) are compared in (d). The 0.03% probability that the difference in mean fluorescence of positive and negative populations could arise by chance is shown by the horizontal dotted line in (b) and (d).

attempted to detect 5.35 fmol of IgG in an immunoassay. The IgG was successfully detected with an average SNR of 4 (for a sample of 20 particles, data shown in Supporting Information Figure S-1).

## CONCLUSION

We have demonstrated a new method for encoding biomolecular probes, based on fabricating micrometer-sized diffraction gratings. The technology has the potential to provide vast numbers of unique codes, up to  $10^{18}$  for a 50- $\mu\text{m}$  particle using 5 times superimposed 2-D gratings.<sup>23</sup> The particles can be rapidly decoded (in  $<1$  ms) by automated software. The encoded particles are fabricated using basic photolithography and are made from a functional polymer (SU-8) that is compatible with multistep chemical synthesis<sup>25</sup> and multiplexed assays. Statistical analysis of the signal variation from particle to particle in assays indicates that 15–20 replicate measurements are required to achieve a  $>99.97\%$  confidence in the discrimination between positive and negative samples. Biochemical assays carried out on these microparticles exhibit favorable binding kinetics and thermodynamics, allowing small amounts ( $<20$  fmol in 1- $\mu\text{L}$  volume) of target analyte to be detected, thus enabling massively parallel determination of molecular interactions with high sensitivity and accuracy. While manual operation of the combined diffraction/fluorescence microscope described herein requires 10–30 s to analyze each particle, the throughput could be greatly increased by coupling decoding optical hardware to a fluidic system. Since analysis of diffraction can be accomplished in an automated

manner on the millisecond time scale, we anticipate throughput comparable to conventional flow cytometers. We envisage using the same devices for directed sorting of particles during multistep chemical synthesis to provide an integrated system for the high-speed manufacture of encoded libraries of molecules (oligonucleotides, peptides, etc.) and analysis of their molecular interactions.

## ACKNOWLEDGMENT

This project was supported by Research Councils UK through the Basic Technology Programme. We also thank the cleanroom staff at EPFL, Switzerland, for their assistance with fabrication and Andrew Whitton for technical assistance. G.R.B., R.T.R. and J.K.S. contributed equally to this work.

## SUPPORTING INFORMATION AVAILABLE

Detailed experimental protocols for functionalization of SU-8 microparticles with oligonucleotides/antibodies and detection of femtomole quantities of anti-human IgG, as well as schematic representation of the modified microscope setup for simultaneous measurement of diffraction and fluorescence from encoded microparticles. This material is available free of charge via the Internet at <http://pubs.acs.org>.

Received for review September 4, 2007. Accepted November 21, 2007.

AC7018574